Pergamon

*Int. J. Solids Structures* Vol. 33, No. 27, pp. 4079–4100, 1996

0020-7683/96 $15.00 + .00

0020-7683(95)00227-8

# FREE VIBRATIONS OF LAMINATED COMPOSITE NON-CIRCULAR THICK CYLINDRICAL SHELLS

K. SUZUKI, G. SHIKANAI
Faculty of Engineering, Yamagata University, Yonezawa, Japan

and

A. W. LEISSA
Department of Engineering Mechanics, Ohio State University, Columbus, Ohio, U.S.A.

(*Received* 17 *May* 1994; *in revised form* 6 *June* 1995)

**Abstract**—An exact solution procedure is presented for analyzing free vibrations of laminated composite, noncircular thick cylindrical shells. Based on the thick lamination theory considering the shear deformation and rotary inertia, equations of motion and boundary conditions are obtained from the stationary conditions of the Lagrangian (Hamilton's principle).

The equations of motion are solved exactly by using power series expansions for the displacements and rotations of symmetrically laminated, cross-ply shells having both ends freely supported. Frequencies are presented for a set of elliptical cylindrical shells having various laminae stacking sequences. The effects of shear deformation and rotary inertia are discussed by comparing the results from the present theory with those from the classical laminated shell theory (thin laminated shell theory). Copyright © 1996 Elsevier Science Ltd

## 1. INTRODUCTION

Laminated composite shells are becoming increasingly used in structures such as spacecraft, automobiles, pressure vessels and many others because of their high specific strengths and specific stiffnesses. There exist a number of investigations dealing with the free vibrations of laminated composite shallow shells, circular cylindrical shells and conical shells (cf, the publications summarized by Qatu and Leissa, 1991a, 1991b; Singh *et al.*, 1991; and Sividas and Ganesan, 1991). But to the authors' knowledge, no published papers exist for laminated composite, noncircular cylindrical shells, which are among the many important structural components. Furthermore, many works dealing with composite shell vibrations use approximate methods.

The present authors (Suzuki and Leissa, 1985, 1986, 1990) were able to obtain exact solutions for the free vibration characteristics (i.e., frequencies and mode shapes) of homogeneous, isotropic, noncircular cylindrical shells having both ends freely supported.

In the present work, free vibrations of laminated composite, noncircular thick cylindrical shells are studied. Based on the thick lamination theory considering the shear deformation and rotary inertia, equations of motion and boundary conditions are obtained from the stationary conditions of the Lagrangian. The equations of motion are solved exactly by means of a power series expansion for symmetrically laminated, cross-ply shells having both ends freely supported. The method developed here is valid for shells with any cross-sections having at least one axis of symmetry and closed, uniformly convex, smooth curves, although the numerical calculations are actually limited by convergence of power series expansion. The present method is demonstrated for a set of elliptical cylindrical shells, and numerical investigations are performed to show the effects of shear deformation and rotary inertia upon the frequencies by comparing the results from the present theory with those from the classical lamination theory (Suzuki *et al.*, 1994).

## 2. ANALYSIS

### 2.1. *Stress and strain relationships*

Let us consider the free vibrations of a laminated, noncircular, thick cylindrical shell composed of $N$ laminae symmetric about the middle surface. For the shell to be considered here, the center line of the cross-section is a smooth curve. The center line, which is the intersection of the middle surface of the shell with the plane $x' = \text{const.}$ is shown in Fig. 1. The length of the shell is $l = \mu r_0$ where $r_0$ is a representative radius and $1/r$ is the curvature at any point along the center line. The coordinate $x'$-axis is taken along the generator of the middle surface, and the arc length $s$ is measured along the center line of the cross-section (the center line and the generator being orthogonal) and the $z$-axis in the direction normal to the middle surface (positive outward). Employ a nondimensional coordinate $x = x'/r_0$ and denote the displacements in the $x'$, $s$ and $z$ directions by $\bar{u}$, $\bar{v}$ and $\bar{w}$, respectively.

The transformation of variable

$$\frac{d\theta}{ds} = \frac{1}{r} = \frac{G}{r_0}\Phi(\theta) \tag{1}$$

is now introduced, where $\theta$ is a variable that denotes an angle between the tangent at the origin of $s$ and the one at any point on the center line, $G$ is a constant determined by the shape of the curve and $\Phi(\theta)$ is a function of $\theta$. The displacements $\bar{u}$, $\bar{v}$ and $\bar{w}$ are assumed in the form

$$\begin{aligned} \bar{u} &= u(x,\theta,t) + \frac{z}{r_0}\Psi_x(x,\theta,t) \\ \bar{v} &= v(x,\theta,t) + \frac{z}{r_0}\Psi_\theta(x,\theta,t) \\ \bar{w} &= w(x,\theta,t) \end{aligned} \tag{2}$$

where $t$ denotes the time, and $u$, $v$, $w$, $\Psi_x$ and $\Psi_\theta$ are functions of $x$, $\theta$ and $t$. The normal and the shearing strain expressions at any point are obtained from Love (1927):

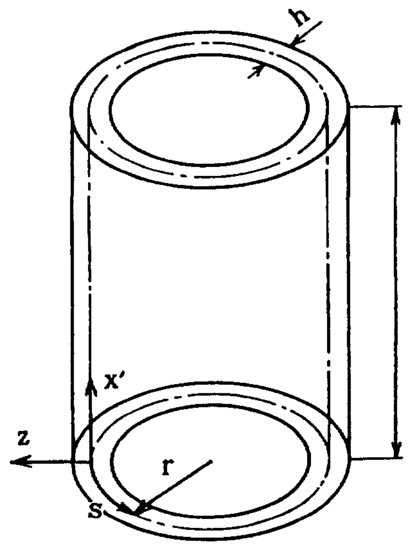


Fig. 1. Coordinates.

$$\varepsilon_{xx} = \frac{1}{r_0}\frac{\partial \bar{u}}{\partial x}, \quad \varepsilon_{\theta\theta} = \frac{1}{r+z}\left(\frac{\partial \bar{v}}{\partial \theta} + \bar{w}\right),$$

$$\varepsilon_{zz} = \frac{\partial \bar{w}}{\partial z}, \quad \varepsilon_{x\theta} = \frac{1}{r_0}\frac{\partial \bar{v}}{\partial x} + \frac{1}{r+z}\frac{\partial \bar{u}}{\partial \theta},$$

$$\varepsilon_{xz} = \frac{\partial \bar{u}}{\partial z} + \frac{1}{r_0}\frac{\partial \bar{w}}{\partial z}, \quad \varepsilon_{\theta z} = \frac{\partial \bar{v}}{\partial z} + \frac{1}{r+z}\left(\frac{\partial \bar{w}}{\partial \theta} - \bar{v}\right). \tag{3}$$

Substituting eqn (2) into eqn (3) yields

$$\varepsilon_{xx} = \frac{1}{r_0}\left(\frac{\partial u}{\partial x} + \frac{z}{r_0}\frac{\partial \Psi_x}{\partial x}\right),$$

$$\varepsilon_{\theta\theta} = \frac{1}{r+z}\left(\frac{\partial v}{\partial \theta} + w + \frac{z}{r_0}\frac{\partial \Psi_\theta}{\partial \theta}\right),$$

$$\varepsilon_{zz} = 0,$$

$$\varepsilon_{xz} = \frac{1}{r_0}\left(\frac{\partial w}{\partial x} + \Psi_x\right),$$

$$\varepsilon_{\theta z} = \frac{1}{r+z}\left(\frac{\partial w}{\partial \theta} - v + \frac{r}{r_0}\Psi_\theta\right),$$

$$\varepsilon_{x\theta} = \frac{1}{r+z}\left(\frac{\partial u}{\partial \theta} + \frac{z}{r_0}\frac{\partial \Psi_x}{\partial \theta}\right) + \frac{1}{r_0}\left(\frac{\partial v}{\partial x} + \frac{z}{r_0}\frac{\partial \Psi_\theta}{\partial x}\right). \tag{4}$$

Consider now that the materials of each lamina consist of parallel, continuous fibers of one material bonded in a matrix material. Each lamina may be regarded on a macroscopic scale as being homogeneous and orthotropic. The stress-strain relation for the $k$th lamina may be written as (cf. Whitney, 1987; Vinson and Sierakowski, 1987), wherein $\sigma_{zz}$ is assumed to be negligible

$$\begin{bmatrix} \sigma_{xx} \\ \sigma_{\theta\theta} \\ \sigma_{\theta z} \\ \sigma_{xz} \\ \sigma_{x\theta} \end{bmatrix}_k = \begin{bmatrix} \bar{Q}_{11} & \bar{Q}_{12} & 0 & 0 & \bar{Q}_{16} \\ \bar{Q}_{12} & \bar{Q}_{22} & 0 & 0 & \bar{Q}_{26} \\ 0 & 0 & \bar{Q}_{44} & \bar{Q}_{45} & 0 \\ 0 & 0 & \bar{Q}_{45} & \bar{Q}_{55} & 0 \\ \bar{Q}_{16} & \bar{Q}_{26} & 0 & 0 & \bar{Q}_{66} \end{bmatrix}_k \begin{bmatrix} \varepsilon_{xx} \\ \varepsilon_{\theta\theta} \\ \varepsilon_{\theta z} \\ \varepsilon_{xz} \\ \varepsilon_{x\theta} \end{bmatrix}_k \tag{5}$$

where $\sigma_{xx}$, $\sigma_{\theta\theta}$ and $\sigma_{zz}$ are normal stress components, and $\sigma_{\theta z}$, $\sigma_{xz}$ and $\sigma_{x\theta}$ are shear stress components. The constants $\bar{Q}_{ij}$ are the elastic stiffness coefficients for the material which are given in Appendix A.

### 2.2. *Lagrangian formulation for vibration*

The strain energy for the $k$th lamina is

$$U_k = \frac{1}{2}\int_{h_{k-1}}^{h_k}\int_{\theta_1}^{\theta_2}\int_0^{l/r_0} [\sigma_{xx}\varepsilon_{xx} + \sigma_{\theta\theta}\varepsilon_{\theta\theta} + \sigma_{\theta z}\varepsilon_{\theta z} + \sigma_{xz}\varepsilon_{xz} + \sigma_{x\theta}\varepsilon_{x\theta}] r_0(r+z)\,\mathrm{d}x\,\mathrm{d}\theta\,\mathrm{d}z \tag{6}$$

where $h_k$ and $h_{k-1}$ are the distances measured from the middle surface to the outer and

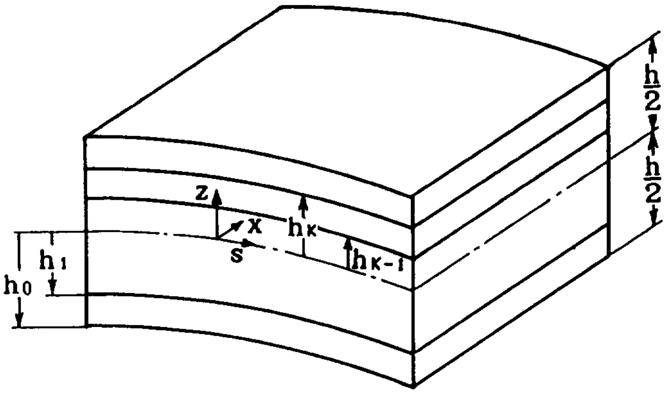


Fig. 2. Cross sectional view of shell.

inner surfaces of the $k$th laminate, respectively, as shown in Fig. 2. The kinetic energy for each lamina is

$$T_k = \frac{1}{2}\iiint \rho^{(k)}\left[\left(\frac{\partial \bar{u}}{\partial t}\right)^2 + \left(\frac{\partial \bar{v}}{\partial t}\right)^2 + \left(\frac{\partial \bar{w}}{\partial t}\right)^2\right] r_0(r+z)\,\mathrm{d}x\,\mathrm{d}\theta\,\mathrm{d}z \tag{7}$$

where $\rho^{(k)}$ is the density of the $k$th lamina per unit volume.

Now define the Lagrangian at any instant of time as follows:

$$L_k = T_k - U_k \tag{8}$$

The Lagrangian of the entire shell is then found to be:

$$L = \sum_{k=1}^{N} L_k \tag{9}$$

where $N$ is the total number of laminae. Substituting eqns (2), (4) and (5) into eqns (6)–(9) and using the following relations

$$\int_{h_{k-1}}^{h_k} \frac{1}{r+z}\,\mathrm{d}z \fallingdotseq \frac{H_1}{r} - \frac{H_2}{r^2} + \frac{H_3}{r^3},$$

$$\int_{h_{k-1}}^{h_k} \frac{z}{r+z}\,\mathrm{d}z \fallingdotseq \frac{H_2}{r} - \frac{H_3}{r^2},$$

$$\int_{h_{k-1}}^{h_k} \frac{z^2}{r+z}\,\mathrm{d}z \fallingdotseq \frac{H_3}{r},$$

$$\int_{h_{k-1}}^{h_k} \frac{z^3}{r+z}\,\mathrm{d}z \fallingdotseq \int_{h_{k-1}}^{h_k} \frac{z^4}{r+z}\,\mathrm{d}z \fallingdotseq 0,$$

$$H_1 = h_k - h_{k-1}, \quad H_2 = \tfrac{1}{2}(h_k^2 - h_{k-1}^2),$$

$$H_3 = \tfrac{1}{3}(h_k^3 - h_{k-1}^3) \tag{10}$$

eqn (9) becomes

$$
\begin{aligned}
-L\bigg/\frac{E_0h^3}{2Gr_0^2} = \iint\bigg[\!\!\bigg[ & -\lambda^4\bigg(\bar{\rho}_1\bigg\{\left(\frac{\partial u}{\partial t}\right)^2+\left(\frac{\partial v}{\partial t}\right)^2+\left(\frac{\partial w}{\partial t}\right)^2\bigg\} \\
& +\frac{1}{\beta}\bar{\rho}_2\bigg[G\Phi\bigg\{\left(\frac{\partial u}{\partial t}\right)^2+\left(\frac{\partial v}{\partial t}\right)^2+\left(\frac{\partial w}{\partial t}\right)^2\bigg\} \\
& +2\left(\frac{\partial u}{\partial t}\frac{\partial \Psi_x}{\partial t}+\frac{\partial v}{\partial t}\frac{\partial \Psi_\theta}{\partial t}\right)\bigg] \\
& +\frac{1}{\beta^2}\bar{\rho}_3\bigg\{\left(\frac{\partial \Psi_x}{\partial t}\right)^2+\left(\frac{\partial \Psi_\theta}{\partial t}\right)^2 \\
& +2G\Phi\left(\frac{\partial u}{\partial t}\frac{\partial \Psi_x}{\partial t}+\frac{\partial v}{\partial t}\frac{\partial \Psi_\theta}{\partial t}\right)\bigg\}\bigg) \\
& +\beta^2\bigg[A_{11}\left(\frac{\partial u}{\partial x}\right)^2+2A_{12}G\Phi\frac{\partial u}{\partial x}\left(\frac{\partial v}{\partial \theta}+w\right) \\
& +A_{22}(G\Phi)^2\left(\frac{\partial v}{\partial \theta}+w\right)^2+A_{44}\bigg\{G\Phi\left(\frac{\partial w}{\partial \theta}-v\right)+\Psi_\theta\bigg\}^2 \\
& +A_{55}\left(\frac{\partial w}{\partial x}+\Psi_x\right)^2+A_{66}\left(G\Phi\frac{\partial u}{\partial \theta}+\frac{\partial v}{\partial x}\right)^2\bigg] \\
& +2\beta^2\bigg[A_{16}\left(G\Phi\frac{\partial u}{\partial x}\frac{\partial u}{\partial \theta}+\frac{\partial u}{\partial x}\frac{\partial v}{\partial x}\right) \\
& +A_{26}\bigg\{(G\Phi)^2\frac{\partial u}{\partial \theta}\left(\frac{\partial v}{\partial \theta}+w\right)+G\Phi\frac{\partial v}{\partial x}\left(\frac{\partial v}{\partial \theta}+w\right)\bigg\} \\
& +A_{45}\left(\frac{\partial w}{\partial x}+\Psi_x\right)\bigg\{G\Phi\left(\frac{\partial w}{\partial \theta}-v\right)+\Psi_\theta\bigg\}\bigg] \\
& +\beta\bigg[B_{11}\bigg\{G\Phi\left(\frac{\partial u}{\partial x}\right)^2+2\frac{\partial u}{\partial x}\frac{\partial \Psi_x}{\partial x}\bigg\} \\
& +B_{22}(G\Phi)^2\bigg\{-G\Phi\left(\frac{\partial v}{\partial \theta}+w\right)^2+2\frac{\partial \Psi_\theta}{\partial \theta}\left(\frac{\partial v}{\partial \theta}+w\right)\bigg\} \\
& -B_{44}G\Phi\bigg\{G\Phi\left(\frac{\partial w}{\partial \theta}-v\right)+\Psi_\theta\bigg\}^2+B_{55}G\Phi\left(\frac{\partial w}{\partial x}+\Psi_x\right)^2 \\
& +B_{66}\bigg\{-(G\Phi)^3\left(\frac{\partial u}{\partial \theta}\right)^2+G\Phi\left(\frac{\partial v}{\partial x}\right)^2 \\
& +2\left(G^2\Phi^2\frac{\partial u}{\partial \theta}\frac{\partial \Psi_x}{\partial \theta}+\frac{\partial v}{\partial x}\frac{\partial \Psi_\theta}{\partial x}\right) \\
& +2G\Phi\left(\frac{\partial u}{\partial \theta}\frac{\partial \Psi_\theta}{\partial x}+\frac{\partial v}{\partial x}\frac{\partial \Psi_x}{\partial \theta}\right)\bigg\}\bigg] \\
& +2\beta\bigg(\bigg[B_{12}G\Phi\bigg\{\frac{\partial u}{\partial x}\frac{\partial \Psi_\theta}{\partial \theta}+\frac{\partial \Psi_x}{\partial x}\left(\frac{\partial v}{\partial \theta}+w\right)\bigg\}
\end{aligned}
$$

$$+B_{16}\left\{G\Phi\left(\frac{\partial u}{\partial x}\frac{\partial \Psi_x}{\partial \theta}+\frac{\partial u}{\partial \theta}\frac{\partial \Psi_x}{\partial x}+\frac{\partial u}{\partial x}\frac{\partial v}{\partial x}\right)\right.$$

$$\left.+\frac{\partial u}{\partial x}\frac{\partial \Psi_\theta}{\partial x}+\frac{\partial v}{\partial x}\frac{\partial \Psi_x}{\partial x}\right\}$$

$$+B_{26}\left[\left\{-(G\Phi)^3\frac{\partial u}{\partial \theta}\left(\frac{\partial v}{\partial \theta}+w\right)\right\}\right.$$

$$+G^2\Phi^2\left\{\frac{\partial \Psi_x}{\partial \theta}\left(\frac{\partial v}{\partial \theta}+w\right)+\frac{\partial u}{\partial \theta}\frac{\partial \Psi_\theta}{\partial \theta}\right\}$$

$$\left.\left.+G\Phi\left\{\frac{\partial \Psi_\theta}{\partial x}\left(\frac{\partial v}{\partial \theta}+w\right)+\frac{\partial v}{\partial x}\frac{\partial \Psi_\theta}{\partial \theta}\right\}\right]\right)$$

$$+D_{11}\left[\left(\frac{\partial \Psi_x}{\partial x}\right)^2+2G\Phi\frac{\partial u}{\partial x}\frac{\partial \Psi_x}{\partial x}\right]$$

$$+D_{22}(G\Phi)^2\left[G\Phi\left(\frac{\partial v}{\partial \theta}+w\right)-\frac{\partial \Psi_\theta}{\partial \theta}\right]^2$$

$$+D_{44}(G\Phi)^2\left[G\Phi\left(\frac{\partial w}{\partial \theta}-v\right)+\Psi_\theta\right]^2$$

$$+D_{66}\left[\left(\frac{\partial \Psi_\theta}{\partial x}\right)^2+G^2\Phi^2\left(\frac{\partial \Psi_x}{\partial \theta}-G\Phi\frac{\partial u}{\partial \theta}\right)^2\right.$$

$$\left.+2G\Phi\left(\frac{\partial \Psi_x}{\partial \theta}\frac{\partial \Psi_\theta}{\partial x}+\frac{\partial v}{\partial x}\frac{\partial \Psi_\theta}{\partial x}\right)\right]+2D_{12}G\Phi\frac{\partial \Psi_x}{\partial x}\frac{\partial \Psi_\theta}{\partial \theta}$$

$$+2D_{16}\left[G\Phi\left(\frac{\partial u}{\partial x}\frac{\partial \Psi_\theta}{\partial x}+\frac{\partial v}{\partial x}\frac{\partial \Psi_x}{\partial x}+\frac{\partial \Psi_x}{\partial x}\frac{\partial \Psi_x}{\partial \theta}\right)\right.$$

$$\left.+\frac{\partial \Psi_x}{\partial x}\frac{\partial \Psi_\theta}{\partial x}\right]+2D_{26}\left[(G\Phi)^4\frac{\partial u}{\partial \theta}\left(\frac{\partial v}{\partial \theta}+w\right)\right.$$

$$-(G\Phi)^3\left\{\frac{\partial \Psi_x}{\partial \theta}\left(\frac{\partial v}{\partial \theta}+w\right)+\frac{\partial u}{\partial \theta}\frac{\partial \Psi_\theta}{\partial \theta}\right\}$$

$$\left.\left.+(G\Phi)^2\frac{\partial \Psi_\theta}{\partial \theta}\frac{\partial \Psi_x}{\partial \theta}+G\Phi\frac{\partial \Psi_\theta}{\partial \theta}\frac{\partial \Psi_\theta}{\partial x}\right]\right]\left(\frac{1}{\Phi}\right)\mathrm{d}x\,\mathrm{d}\theta \tag{11}$$

where $h$ is the total shell thickness, $\rho_0$ and $E_0$ are a representative material density and elastic modulus, respectively, and

$$\lambda^4=\frac{\rho_0 r_0^4}{E_0 h^2},\quad \beta=\frac{r_0}{h},\quad \bar{\rho}_1=\sum_{k=1}^{N}\frac{\rho^{(k)}}{\rho_0}(h_k-h_{k-1})/h,$$

$$\bar{\rho}_2=\sum_{k=1}^{N}\frac{1}{2}\frac{\rho^{(k)}}{\rho_0}(h_k^2-h_{k-1}^2)/h^2,$$

$$\bar{\rho}_3=\sum_{k=1}^{N}\frac{1}{3}\frac{\rho^{(k)}}{\rho_0}(h_k^3-h_{k-1}^3)/h^3,$$

$$A_{ij} = \sum_{k=1}^{N} \frac{\bar{Q}_{ij}^{(k)}}{E_0}(h_k - h_{k-1})/h,$$

$$B_{ij} = \sum_{k=1}^{N} \frac{1}{2}\frac{\bar{Q}_{ij}^{(k)}}{E_0}(h_k^2 - h_{k-1}^2)/h^2,$$

$$D_{ij} = \sum_{k=1}^{N} \frac{1}{3}\frac{\bar{Q}_{ij}^{(k)}}{E_0}(h_k^3 - h_{k-1}^3)/h^3. \tag{12}$$

For a cross-ply laminate of orthotropic laminae oriented at either 0° or 90° to the laminate axes, $A_{16}$, $A_{26}$, $A_{45}$, $B_{16}$, $B_{26}$, $D_{16}$ and $D_{26}$ in eqn (11) are zero. For shells which are laminated symmetrically with respect to the midsurfaces, $\bar{\rho}_2$ and $B_{ij} = 0$.

### 2.3. *Equations of motion and boundary conditions*

Applying Hamilton's principle $\delta \int_{t_1}^{t_2} L\,\mathrm{d}t = 0$, one obtains

$$\begin{aligned}
&-\int_{t_1}^{t_2}\int_{\theta_1}^{\theta_2}\int_0^{\mu}[E_1\delta u + E_2\delta v + E_3\delta w + E_4\delta\Psi_x + E_5\delta\Psi_\theta]\,\mathrm{d}x\,\mathrm{d}\theta\,\mathrm{d}t \\
&+\int_{t_1}^{t_2}\int_0^{\mu}[T_1\delta u + T_2\delta v + T_3\delta w + M_1\delta\Psi_x + M_2\delta\Psi_\theta]|_{\theta=\theta_1}^{\theta=\theta_2}\,\mathrm{d}x\,\mathrm{d}t \\
&+\int_{t_1}^{t_2}\int_{\theta_1}^{\theta_2}[T_4\delta u + T_5\delta v + T_6\delta w + M_3\delta\Psi_x + M_4\delta\Psi_\theta]|_{x=0}^{x=\mu}\,\mathrm{d}\theta\,\mathrm{d}t \\
&-\int_{\theta_1}^{\theta_2}\int_0^{\mu}\lambda^4\Bigg[\left\{\bar{\rho}_1\frac{\partial u}{\partial t} + \frac{\bar{\rho}_2}{\beta}\left(G\Phi\frac{\partial u}{\partial t} + \frac{\partial \Psi_x}{\partial t}\right) + \frac{\bar{\rho}_3}{\beta^2}G\Phi\frac{\partial \Psi_x}{\partial t}\right\}\delta u \\
&+\left\{\bar{\rho}_1\frac{\partial v}{\partial t} + \frac{\bar{\rho}_2}{\beta}\left(G\Phi\frac{\partial v}{\partial t} + \frac{\partial \Psi_\theta}{\partial t}\right) + \frac{\bar{\rho}_3}{\beta^2}G\Phi\frac{\partial \Psi_\theta}{\partial t}\right\}\delta v + \left\{\bar{\rho}_1 + \frac{\bar{\rho}_2}{\beta}G\Phi\right\}\frac{\partial w}{\partial t}\delta w \\
&+\left\{\frac{\bar{\rho}_2}{\beta}\frac{\partial u}{\partial t} + \frac{\bar{\rho}_3}{\beta^2}\left(\frac{\partial \Psi_x}{\partial t} + G\Phi\frac{\partial u}{\partial t}\right)\right\}\delta\Psi_x \\
&+\left\{\frac{\bar{\rho}_2}{\beta}\frac{\partial v}{\partial t} + \frac{\bar{\rho}_3}{\beta^2}\left(\frac{\partial \Psi_\theta}{\partial t} + G\Phi\frac{\partial v}{\partial t}\right)\right\}\delta\Psi_\theta\Bigg]\Bigg|_{t=t_1}^{t=t_2}\left(\frac{1}{\Phi}\right)\mathrm{d}x\,\mathrm{d}\theta = 0
\end{aligned} \tag{13}$$

where

$$E_1 = -\lambda^4\left[\bar{\rho}_1\frac{\partial^2}{\partial t^2}\left(\frac{u}{\Phi}\right) + \frac{\bar{\rho}_2}{\beta}\left\{G\frac{\partial^2 u}{\partial t^2} + \frac{\partial^2}{\partial t^2}\left(\frac{\Psi_x}{\Phi}\right)\right\} + \frac{\bar{\rho}_3 G}{\beta^2}\frac{\partial^2 \Psi_x}{\partial t^2}\right] + \frac{\partial T_1}{\partial \theta} + \frac{\partial T_4}{\partial x},$$

$$E_2 = -\lambda^4\left[\bar{\rho}_1\frac{\partial^2}{\partial t^2}\left(\frac{v}{\Phi}\right) + \frac{\bar{\rho}_2}{\beta}\left\{G\frac{\partial^2 v}{\partial t^2} + \frac{\partial^2}{\partial t^2}\left(\frac{\Psi_\theta}{\Phi}\right)\right\} + \frac{\bar{\rho}_3 G}{\beta^2}\frac{\partial^2 \Psi_\theta}{\partial t^2}\right] + T_3 + \frac{\partial T_2}{\partial \theta} + \frac{\partial T_5}{\partial x},$$

$$E_3 = -\lambda^4\left\{\bar{\rho}_1\frac{\partial^2}{\partial t^2}\left(\frac{w}{\Phi}\right) + \bar{\rho}_2\frac{G}{\beta}\frac{\partial^2 w}{\partial t^2}\right\} - T_2 + \frac{\partial T_3}{\partial \theta} + \frac{\partial T_6}{\partial x},$$

$$E_4 = -\lambda^4\left[\frac{\bar{\rho}_2}{\beta}\frac{\partial^2}{\partial t^2}\left(\frac{u}{\Phi}\right) + \frac{\bar{\rho}_3}{\beta^2}\left\{\frac{\partial^2}{\partial t^2}\left(\frac{\Psi_x}{\Phi}\right) + G\frac{\partial^2 u}{\partial t^2}\right\}\right] + \frac{\partial M_1}{\partial \theta} + \frac{\partial M_3}{\partial x} - T_6,$$

$$E_5 = -\lambda^4\left[\frac{\bar{\rho}_2}{\beta}\frac{\partial^2}{\partial t^2}\left(\frac{v}{\Phi}\right)+\frac{\bar{\rho}_3}{\beta^2}\left\{\frac{\partial^2}{\partial t^2}\left(\frac{\Psi_\theta}{\Phi}\right)+G\frac{\partial^2 v}{\partial t^2}\right\}\right]+\frac{\partial M_2}{\partial\theta}+\frac{\partial M_4}{\partial x}-\frac{T_3}{G\Phi} \tag{14}$$

and where

$$\begin{aligned}
T_1 = {} & \beta^2 G\left[A_{66}\left(G\Phi\frac{\partial u}{\partial\theta}+\frac{\partial v}{\partial x}\right)+A_{16}\frac{\partial u}{\partial x}+A_{26}G\Phi\left(\frac{\partial v}{\partial\theta}+w\right)\right] \\
& -\beta G\left[B_{66}\left(G^2\Phi^2\frac{\partial u}{\partial\theta}-G\Phi\frac{\partial\Psi_x}{\partial\theta}-\frac{\partial\Psi_\theta}{\partial x}\right)-B_{16}\frac{\partial\Psi_x}{\partial x}\right. \\
& \left.+B_{26}\left\{G^2\Phi^2\left(\frac{\partial v}{\partial\theta}+w\right)-G\Phi\frac{\partial\Psi_\theta}{\partial\theta}\right\}\right] \\
& -G\left[D_{66}G^2\Phi^2\left(\frac{\partial\Psi_x}{\partial\theta}-G\Phi\frac{\partial u}{\partial\theta}\right)-D_{26}\left\{G^3\Phi^3\left(\frac{\partial v}{\partial\theta}+w\right)-G^2\Phi^2\frac{\partial\Psi_\theta}{\partial\theta}\right\}\right], \\
T_2 = {} & \beta^2 G\left[A_{12}\frac{\partial u}{\partial x}+A_{22}G\Phi\left(\frac{\partial v}{\partial\theta}+w\right)+A_{26}\left(G\Phi\frac{\partial u}{\partial\theta}+\frac{\partial v}{\partial x}\right)\right] \\
& -\beta G\left[B_{22}G\Phi\left\{G\Phi\left(\frac{\partial v}{\partial\theta}+w\right)-\frac{\partial\Psi_\theta}{\partial\theta}\right\}-B_{12}\frac{\partial\Psi_x}{\partial x}+B_{26}\left(G^2\Phi^2\frac{\partial u}{\partial\theta}-G\Phi\frac{\partial\Psi_x}{\partial\theta}-\frac{\partial\Psi_\theta}{\partial x}\right)\right] \\
& +G\left[D_{22}G^2\Phi^2\left\{G\Phi\left(\frac{\partial v}{\partial\theta}+w\right)-\frac{\partial\Psi_\theta}{\partial\theta}\right\}+D_{26}G^2\Phi^2\left(G\Phi\frac{\partial u}{\partial\theta}-\frac{\partial\Psi_x}{\partial\theta}\right)\right], \\
T_3 = {} & \beta^2 G\left[A_{44}\left\{G\Phi\left(\frac{\partial w}{\partial\theta}-v\right)+\Psi_\theta\right\}+A_{45}\left(\frac{\partial w}{\partial x}+\Psi_x\right)\right] \\
& -\beta G\left[B_{44}G\Phi\left\{G\Phi\left(\frac{\partial w}{\partial\theta}-v\right)+\Psi_\theta\right\}\right]+G\left[D_{44}G^2\Phi^2\left\{G\Phi\left(\frac{\partial w}{\partial\theta}-v\right)+\Psi_\theta\right\}\right], \\
T_4 = {} & \beta^2\left[A_{11}\frac{1}{\Phi}\frac{\partial u}{\partial x}+A_{12}G\left(\frac{\partial v}{\partial\theta}+w\right)+A_{16}\left(G\frac{\partial u}{\partial\theta}+\frac{1}{\Phi}\frac{\partial v}{\partial x}\right)\right] \\
& +\beta\left[B_{11}\left(G\frac{\partial u}{\partial x}+\frac{1}{\Phi}\frac{\partial\Psi_x}{\partial x}\right)+B_{12}G\frac{\partial\Psi_\theta}{\partial\theta}+B_{16}\left\{G\left(\frac{\partial\Psi_x}{\partial\theta}+\frac{\partial v}{\partial x}\right)+\frac{1}{\Phi}\frac{\partial\Psi_\theta}{\partial x}\right\}\right] \\
& +D_{11}G\frac{\partial\Psi_x}{\partial x}+D_{16}G\frac{\partial\Psi_\theta}{\partial x}, \\
T_5 = {} & \beta^2\left[A_{66}\left(G\frac{\partial u}{\partial\theta}+\frac{1}{\Phi}\frac{\partial v}{\partial x}\right)+A_{16}\frac{1}{\Phi}\frac{\partial u}{\partial x}+A_{26}G\left(\frac{\partial v}{\partial\theta}+w\right)\right] \\
& +\beta\left[B_{66}\left(G\frac{\partial v}{\partial x}+\frac{1}{\Phi}\frac{\partial\Psi_\theta}{\partial x}+G\frac{\partial\Psi_x}{\partial\theta}\right)+B_{16}\left(G\frac{\partial u}{\partial x}+\frac{1}{\Phi}\frac{\partial\Psi_x}{\partial x}\right)+B_{26}G\frac{\partial\Psi_\theta}{\partial\theta}\right] \\
& +D_{66}G\frac{\partial\Psi_\theta}{\partial x}+D_{16}G\frac{\partial\Psi_x}{\partial x}, \\
T_6 = {} & \beta^2\left[A_{55}\frac{1}{\Phi}\left(\frac{\partial w}{\partial x}+\Psi_x\right)+A_{45}\left\{G\left(\frac{\partial w}{\partial\theta}-v\right)+\frac{\Psi_\theta}{\Phi}\right\}\right] \\
& +\beta B_{55}G\left(\frac{\partial w}{\partial x}+\Psi_x\right),
\end{aligned}$$

$$M_1 = \beta G\left[B_{66}\left(G\Phi\frac{\partial u}{\partial\theta}+\frac{\partial v}{\partial x}\right)+B_{16}\frac{\partial u}{\partial x}+B_{26}G\Phi\left(\frac{\partial v}{\partial\theta}+w\right)\right]$$
$$+G\left[D_{66}\left\{G\Phi\left(\frac{\partial\Psi_x}{\partial\theta}-G\Phi\frac{\partial u}{\partial\theta}\right)+\frac{\partial\Psi_\theta}{\partial x}\right\}+D_{16}\frac{\partial\Psi_x}{\partial x}-D_{26}\left\{G^2\Phi^2\left(\frac{\partial v}{\partial\theta}+w\right)-G\Phi\frac{\partial\Psi_\theta}{\partial\theta}\right\}\right],$$

$$M_2 = \beta G\left[B_{22}G\Phi\left(\frac{\partial v}{\partial\theta}+w\right)+B_{12}\frac{\partial u}{\partial x}+B_{26}\left(G\Phi\frac{\partial u}{\partial\theta}+\frac{\partial v}{\partial x}\right)\right]$$
$$-G\left[D_{22}G\Phi\left\{G\Phi\left(\frac{\partial v}{\partial\theta}+w\right)-\frac{\partial\Psi_\theta}{\partial\theta}\right\}-D_{12}\frac{\partial\Psi_x}{\partial x}+D_{26}\left(G^2\Phi^2\frac{\partial u}{\partial\theta}-G\Phi\frac{\partial\Psi_x}{\partial\theta}-\frac{\partial\Psi_\theta}{\partial x}\right)\right],$$

$$M_3 = \beta\left[B_{11}\frac{1}{\Phi}\frac{\partial u}{\partial x}+B_{12}G\left(\frac{\partial v}{\partial\theta}+w\right)+B_{16}\left(G\frac{\partial u}{\partial\theta}+\frac{1}{\Phi}\frac{\partial v}{\partial x}\right)\right]$$
$$+D_{11}\left(\frac{1}{\Phi}\frac{\partial\Psi_x}{\partial x}+G\frac{\partial u}{\partial x}\right)+D_{12}G\frac{\partial\Psi_\theta}{\partial\theta}+D_{16}\left\{G\left(\frac{\partial v}{\partial x}+\frac{\partial\Psi_x}{\partial\theta}\right)+\frac{1}{\Phi}\frac{\partial\Psi_\theta}{\partial x}\right\},$$

$$M_4 = \beta\left[B_{66}\left(G\frac{\partial u}{\partial\theta}+\frac{1}{\Phi}\frac{\partial v}{\partial x}\right)+B_{16}\frac{1}{\Phi}\frac{\partial u}{\partial x}+B_{26}G\left(\frac{\partial v}{\partial\theta}+w\right)\right]$$
$$+D_{66}\left\{\frac{1}{\Phi}\frac{\partial\Psi_\theta}{\partial x}+G\left(\frac{\partial\Psi_x}{\partial\theta}+\frac{\partial v}{\partial x}\right)\right\}+D_{16}\left(G\frac{\partial u}{\partial x}+\frac{1}{\Phi}\frac{\partial\Psi_x}{\partial x}\right)+D_{26}G\frac{\partial\Psi_\theta}{\partial\theta}. \tag{15}$$

Euler's equations (equations of motion) are

$$E_1 = E_2 = E_3 = E_4 = E_5 = 0 \tag{16}$$

The boundary conditions at $\theta = \theta_1$ and $\theta = \theta_2$ are

$$T_1\delta u = T_2\delta v = T_3\delta w = M_1\delta\Psi_x = M_2\delta\Psi_\theta = 0 \tag{17}$$

For boundaries at $x = 0$ and $x = \mu$ they are

$$T_4\delta u = T_5\delta v = T_6\delta w = M_3\delta\Psi_x = M_4\delta\Psi_\theta = 0 \tag{18}$$

The last term in eqn (13) vanishes because of the additional conditions of displacement, $\delta u = \delta v = \delta w = \delta\Psi_x = \delta\Psi_\theta = 0$ at $t = t_1$ and $t = t_2$.

Replacing $w$, $\Psi_x$ and $\Psi_\theta$ by $(-w)$, $(-\Psi_x)$ and $(-\Psi_\theta)$, respectively and setting

$$A_{11} = A_{22} = 12,\quad A_{12} = 12(1-2\zeta),\quad A_{44} = A_{55} = 12\kappa'\zeta$$
$$A_{66} = 12\zeta,\quad D_{11} = D_{22} = 1,\quad D_{12} = 1-2\zeta,\quad D_{44} = \kappa'\zeta,\quad D_{66} = \zeta = 1-2v$$
$$E_0 = E/12(1-v^2),\quad \lambda^4\bar{\rho}_1 = \alpha^4,\quad \lambda^4\bar{\rho}_3/\beta^2 = \alpha^4/\beta,\quad 12\beta^2 = \beta \tag{19}$$

one finds that eqns (13)–(18) correspond with those for a homogeneous, isotropic, non-circular thick cylindrical shell obtained by Suzuki and Leissa (1990).

### 2.4. *Solutions of the equation of motion for freely supported ends*

Consider the vibration of a symmetrically laminated, cross-ply noncircular cylindrical shell having the curved ends supported by shear diaphragms (or freely supported). As mentioned at the end of Section 2.2, for this lamination type, $A_{16} = A_{26} = A_{45} = D_{16} = D_{26} = 0$, $\bar{\rho}_2 = 0$ and all $B_{ij} = 0$. The conditions to be imposed at the ends are

$$T_4 = v = w = M_3 = \Psi_\theta = 0 \tag{20}$$

which satisfy eqns (18). Equations (20) are exactly satisfied at $x = 0$ and $\mu$ by choosing

$$\{u,\Psi_x\} = \{u_m(\theta),\Psi_{xm}(\theta)\}\cos\frac{m\pi}{\mu}x\sin\omega t$$

$$\{v,w,\Psi_\theta\} = \{v_m(\theta),w_m(\theta),\Psi_{\theta m}(\theta)\}\sin\frac{m\pi}{\mu}x\sin\omega t \tag{21}$$

where $m$ is an integer, and $\omega$ is the circular frequency of vibration. Substituting the displacements (21) into the equations of motion (16) yields the following set of ordinary differential equations:

$$\alpha_0^4\left[\bar{\rho}_1\left(\frac{u_m}{\Phi}\right)+\bar{\rho}_3\frac{G}{\beta^2}\Psi_{xm}\right]+\frac{\mathrm{d}T_{1m}}{\mathrm{d}\theta}+KT_{4m}=0,$$

$$\alpha_0^4\left[\bar{\rho}_1 v_m+\bar{\rho}_3\frac{G}{\beta^2}\Phi\Psi_{\theta m}\right]+\Phi\left[T_{3m}+\frac{\mathrm{d}T_{2m}}{\mathrm{d}\theta}-KT_{5m}\right]=0,$$

$$\alpha_0^4\bar{\rho}_1 w_m-\Phi\left[T_{2m}-\frac{\mathrm{d}T_{3m}}{\mathrm{d}\theta}+KT_{6m}\right]=0,$$

$$\alpha_0^4\frac{\bar{\rho}_3}{\beta^2}[\Psi_{xm}+G\Phi u_m]+\Phi\left[\frac{\mathrm{d}M_{1m}}{\mathrm{d}\theta}+KM_{3m}-T_{6m}\right]=0,$$

$$\alpha_0^4\frac{\bar{\rho}_3}{\beta^2}\left[\frac{\Psi_{\theta m}}{\Phi}+Gv_m\right]-\frac{T_{3m}}{G\Phi}+\frac{\mathrm{d}M_{2m}}{\mathrm{d}\theta}-KM_{4m}=0 \tag{22}$$

where

$$\alpha_0^4=\rho_0\omega^2 r_0^4/E_0h^2,\quad \beta=r_0/h,\quad K=m\pi/\mu \tag{23}$$

and $T_{1m}, T_{2m},\ldots, M_{4m}$ are expressions obtained by substituting eqns (21) into $T_1, T_2,\ldots, M_4$ in eqns (15) and omitting $\sin Kx$ or $\cos Kx$. Equations (22) are complicated differential equations with variable coefficients, but exact solutions may be obtained by expressing the function $\Phi^2(\theta)$ as an infinite power series in $\theta$ and assuming solutions for $u_m$, $v_m$, $w_m$, $\Psi_{xm}$, $\Psi_{\theta m}$ which are also infinite power series in $\theta$. The solution procedure will be demonstrated here for shells having cross-sections with one or more axes of symmetry.

Let $\theta = 0$ correspond to a symmetry axis and expand $\Phi^2$ as

$$\Phi^2=\Phi_0\sum_{n=0}^{\infty}\eta_n\theta^{2n} \tag{24}$$

One can denote $\Phi^2$ as in eqn (24) for the curves for which the curvatures are expressed as even functions of $\theta$ (cf. Suzuki *et al.*, 1978). As an example, consider an ellipse for which the equations are denoted by the rectangular coordinates $(\xi_1, \xi_2)$ as $\xi_1 = a\cos\bar{\eta}$, $\xi_2 = b\sin\bar{\eta}$ in which $2a$, $2b$ and $\bar{\eta}$ are the major and the minor axes and a parameter, respectively. Setting the representative radius $r_0$ and the ellipticity of the curve $\mu_0$ as

$$r_0=\sqrt{(a^2+b^2)/2},\quad \mu_0=(a^2-b^2)/(a^2+b^2) \tag{25}$$

one obtains

$$\Phi(\theta) = (1+\mu_0 \cos 2\theta)^{3/2},$$

$$\tan\theta = \sqrt{(1+\mu_0)/(1-\mu_0)}\tan\bar{\eta},$$

$$1/G = 1-\mu_0^2, \quad \Phi_0 = (1+\mu_0)^3, \quad \eta_0 = 1,$$

$$\eta_n = \frac{3\mu_0^3(-1)^n 2^{2n}}{(1+\mu_0)^3(2n)!}\left[\frac{1+3^{2n-1}}{4} + \frac{2^{2n-1}}{\mu_0} + \frac{1}{\mu_0^2}\right]. \tag{26}$$

Equations (22) have two solutions, one in which $u_m/\Phi$, $w_m$ and $\Psi_{xm}$ are even functions of $\theta$, and $v_m$ and $\Psi_{\theta m}/\Phi$ are odd functions of $\theta$, and another in which $u_m/\Phi$, $w_m$ and $\Psi_{xm}$ are odd functions of $\theta$, and $v_m$ and $\Psi_{\theta m}/\Phi$ are even functions of $\theta$.

(i) In the case of that $u_m/\Phi$ is an even function of $\theta$ one takes

$$u_m/\Phi = \sum_{n=0}^{\infty} A_n\theta^{2n}, v_m = \sum_{n=0}^{\infty} B_n\theta^{2n+1}, w_m = \sum_{n=0}^{\infty} C_n\theta^{2n}$$

$$\Psi_{xm} = \sum_{n=0}^{\infty} D_n\theta^{2n}, \Psi_{\theta m}/\Phi = \sum_{n=0}^{\infty} F_n\theta^{2n+1} \tag{27}$$

where $A_n$, $B_n$, $C_n$, $D_n$ and $F_n$ are coefficients which are determined in turn as follows. Substituting eqns (27) into (22) yields

$$\sum_{n=0}^{\infty} [G^2\Phi_0\eta_0(2n+1)(2n+2)\{(\beta^2 A_{66}+G^2\Phi_0\eta_0 D_{66})A_{n-1} - GD_{66}D_{n-1}\} + f_{na}]\theta^{2n} = 0$$

$$\sum_{n=0}^{\infty} [G^2\Phi_0\eta_0(2n+2)(2n+3)\{(\beta^2 A_{22}+G^2\Phi_0\eta_0 D_{22})B_{n+1} - G\Phi_0\eta_0 D_{22}F_{n+1}\} + f_{nb}]\theta^{2n+1} = 0$$

$$\sum_{n=0}^{\infty} [G^2\Phi_0\eta_0(2n+1)(2n+2)(\beta^2 A_{44}+G^2\Phi_0\eta_0 D_{44})C_{n-1} + f_{nc}]\theta^{2n} = 0$$

$$\sum_{n=0}^{\infty} [G^2\Phi_0\eta_0(2n+1)(2n+2)D_{66}(D_{n+1} - G\Phi_0\eta_0 A_{n+1}) + f_{nd}]\theta^{2n} = 0$$

$$\sum_{n=0}^{\infty} [G^2\Phi_0\eta_0(2n+2)(2n+3)D_{22}(-GB_{n-1} + F_{n+1}) + f_{ne}]\theta^{2n+1} = 0 \tag{28}$$

where $f_{na}$, $f_{nb}$, $f_{nc}$, $f_{nd}$ and $f_{ne}$ are series' defined in Appendix B.

(ii) In the case that $u_m/\Phi$ is an odd function of $\theta$ one takes

$$u_m/\Phi = \sum_{n=0}^{\infty} A_n\theta^{2n+1}, \quad v_m = \sum_{n=0}^{\infty} B_n\theta^{2n}, \quad w_m = \sum_{n=0}^{\infty} C_n\theta^{2n+1},$$

$$\Psi_{xm} = \sum_{n=0}^{\infty} D_n\theta^{2n+1}, \quad \Psi_{\theta m}/\Phi = \sum_{n=0}^{\infty} F_n\theta^{2n} \tag{29}$$

where $A_n$, $B_n$, $C_n$, $D_n$ and $F_n$ are undetermined coefficients. Substituting eqns (29) into (22) yields

$$\sum_{n=0}^{\infty} [G^2\Phi_0\eta_0(2n+2)(2n+3)\{(\beta^2 A_{66}+G^2\Phi_0\eta_0 D_{66})A_{n+1} - GD_{66}D_{n+1}\} + f_{na}]\theta^{2n+1} = 0$$

$$\sum_{n=0}^{\infty} [G^2\Phi_0\eta_0(2n+1)(2n+2)\{(\beta^2 A_{22}+G^2\Phi_0\eta_0 D_{22})B_{n+1} - G\Phi_0\eta_0 D_{22}F_{n+1}\} + f_{nb}]\theta^{2n} = 0$$

$$\sum_{n=0}^{\infty} [G^2\Phi_0\eta_0(2n+2)(2n+3)(\beta^2 A_{44}+G^2\Phi_0\eta_0 D_{44})C_{n+1}+f_{nc}]\theta^{2n+1} = 0$$

$$\sum_{n=0}^{\infty} [G^2\Phi_0\eta_0(2n+2)(2n+3)D_{66}(D_{n+1}-G\Phi_0\eta_0 A_{n+1})+f_{nd}]\theta^{2n+1} = 0$$

$$\sum_{n=0}^{\infty} [G^2\Phi_0\eta_0(2n+1)(2n+2)D_{22}(-GB_{n+1}+F_{n+1})+f_{ne}]\theta^{2n} = 0 \tag{30}$$

where $f_{na}, f_{nb}, f_{nc}, f_{nd}$ and $f_{ne}$ are series defined in Appendix B. If eqns (28) and (30) hold for any value of $\theta$, the expressions in the brackets of each equation in eqns (28) and (30) must become zero. Hence, in eqn (28), the coefficients $C_{n+1}$, $(A_{n+1}, D_{n+1})$ and $(B_{n+1}, F_{n+1})$ $(n \geqslant 0)$ are obtained in turn with $A_0$, $B_0$, $C_0$, $D_0$ and $F_0$, left undetermined. In eqn (30), the coefficients $(B_{n+1}, F_{n+1})$, $C_{n+1}$ and $(A_{n+1}, D_{n+1})$ $(n \geqslant 0)$ are obtained in terms of $A_0$, $B_0$, $C_0$, $D_0$ and $F_0$, with the last five left undetermined. In this way, five independent solutions arise from each set of eqns (28) and (30), and ten independent solutions for the complete problem are obtained. The general solutions of eqns (22) are expressed by combining linearly these ten independent solutions. However, when the cross-section is symmetric about $\theta = 0$, the vibrations are divided into a symmetric vibration and an antisymmetric one about the axis of symmetry corresponding to $\theta = 0$. Then the displacements given by eqns (27) are the solutions for the symmetric modes of vibration, and those from eqn (29) are for the antisymmetric modes. Thus the general solutions are expressed by combining linearly the five independent solutions obtained from eqn (27) or (29) as follows:

$$\{u_m, v_m, w_m, \Psi_{xm}, \Psi_{\theta m}\} = \sum_{i=1}^{5} \lambda_i (u_{mi}, v_{mi}, w_{mi}, \Psi_{xmi}, \Psi_{\theta mi}) \tag{31}$$

where $\lambda_1, \cdots, \lambda_5$ are arbitrary constants.

Consider now an elliptical cylindrical shell having a midsurface cross-section as shown in Fig. 3. The axes of symmetry are the $\xi_1$-axis passing through the points $\theta = 0, \pi$ and the $\xi_2$-axis passing through the points $\theta = \pm\pi/2$. Vibrations are divided into four symmetry classes (S-S, S-A, A-S, A-A), depending on whether they are symmetric (S) or antisymmetric (A) with respect to the $\xi_1$- or $\xi_2$-axes, respectively. These symmetry classes are obtained by utilizing the symmetric functions (27) or the antisymmetric functions (29), and by enforcing the conditions at $\theta = \pi/2$ that either

$$T_1 = v = T_3 = M_1 = \Psi_\theta = 0 \quad \text{(symmetric)} \tag{32}$$

or

$$u = T_2 = w = \Psi_x = M_2 = 0 \quad \text{(antisymmetric)} \tag{33}$$

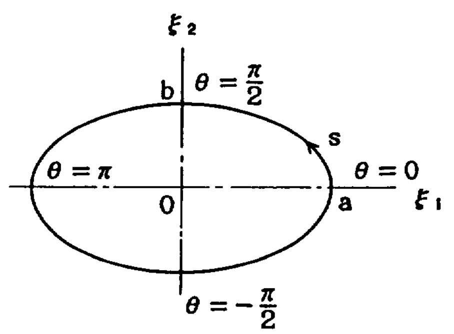


Fig. 3. Elliptical shell.

## 3. NUMERICAL RESULTS

Numerical studies are made for elliptical cylindrical shells of symmetric cross-ply laminates. As composite materials, uni-directional graphite fiber reinforced epoxy (hereafter called G/E) are considered. All layers are taken to be of equal thickness and have equal material density, that is $\rho^{(k)} = \rho_0$. The following moduli of elasticity of the materials are used: $E_{11} = 138$ (GPa), $E_{22} = 8.96$ (GPa), $G_{12} = G_{13} = 7.1$ (GPa), $G_{23} = 3.45$ (GPa), $\nu_{12} = \nu_{13} = \nu_{23} = 0.30$. To be specific, the following shell parameters are used: $\beta\ (=r_0/h) = 6$, $\mu_0 = 0.1, 0.2, 0.3, 0.4$ (corresponding to $a/b = 1.11, 1.22, 1.36, 1.53$).

To show the characteristics of the vibration, the non-dimensional frequency parameter $\alpha_0^4/\beta^2$ is used where, from eqns (23),

$$\frac{\alpha_0^4}{\beta^2} = \frac{\rho_0\omega^2 r_0^2}{E_0} \tag{34}$$

and $E_0$ is defined by $E_0 = E_{11}/\{12(1-\nu_{12}\nu_{21})\}$. In the calculations for the results shown hereafter, $\beta$ and $K(=m\pi r_0/l)$ were first chosen, and then a search was conducted for the values of $\alpha_0^4/\beta^2$ which satisfy the frequency equations.

The displacement functions $u_m$, $v_m$, $w_m$, $\Psi_{xm}$ and $\Psi_{\theta m}$ are calculated by retaining 120 terms for each of the coefficients $A_n$, $B_n$, $C_n$, $D_n$ and $F_n$ in eqns (27) and (29). Each of the independent solutions corresponding to each symmetry class was obtained by setting one of $A_0$, $B_0$, $C_0$, $D_0$ and $F_0$ equal to unity and the others equal to zero.

The accuracy of algebraic calculations was confirmed by comparing the results from eqns (19) and those for homogeneous, isotropic shells from Suzuki and Leissa (1990).

Table 1 shows the convergence of the solutions arising from eqns (27). In the table are shown the number of terms and converged digits of the functions obtained from ($A_0 = 1$, $B_0 = C_0 = D_0 = F_0 = 0$). The rate of convergence of the solutions varies with the parameters. In general, the convergence becomes slow as $\beta$, $\mu_0$, $\alpha_0^4/\beta^2$, $N$ and $K$ become larger. The first two parameters, in particular, have larger influences on the convergence. Table 1 shows how the convergence diminishes as the ellipticity parameter $\mu_0$ increases from 0.2 ($a/b = 1.22$) to 0.4 ($a/b = 1.53$). The convergence of the other four sets of solutions is similar.

Figures 4–7 show the frequency curves of elliptical cylindrical shells with stacking sequence (90°, 0°, 90°) in the case where the number of laminae $N = 3$, $\beta = 6.0$ and $\mu_0 = 0.2$. The curves are for the first, second and third frequencies of vibration in order from below, wherein the frequency parameter $\alpha_0^4/\beta^2$ is plotted versus the length ratio $K$. The numbers on the curves denote the points at which the mode shapes will be shown later in Fig. 10. In Figs 5 and 6, the third mode frequency curves of the classical theory, which are not shown in the figures, have the values from $\alpha_0^4/\beta^2 \fallingdotseq 14$ at $K = 0.25$ to 18 at $K = 4.0$. The curves for

Table 1. Converged digits of functions (S-S) modes, $N = 3$ (90°, 0°, 90°), $\alpha_0^4/\beta^2 = 8.0$, $K = 3$ $\beta = 6.0$

| | Number of terms | | | | | |
|---|---|---|---|---|---|---|
| | $\mu_0 = 0.2$ | | | $\mu_0 = 0.4$ | | |
| Functions | 70 | 80 | 100 | 80 | 100 | 120 |
| $u_m$ | 9 | 12 | 15 | 6 | 7 | 9 |
| $v_m$ | 10 | 13 | 15 | 8 | 8 | 10 |
| $w_m$ | 9 | 12 | 14 | 7 | 7 | 9 |
| $\Psi_{xm}$ | 9 | 12 | 15 | 8 | 7 | 10 |
| $\Psi_{\theta m}$ | 9 | 12 | 15 | 4 | 7 | 7 |
| $T_{1m}$ | 10 | 13 | 15 | 7 | 6 | 10 |
| $T_{2m}$ | 9 | 12 | 15 | 6 | 7 | 9 |
| $T_{3m}$ | 9 | 11 | 15 | 6 | 8 | 9 |
| $M_{1m}$ | 10 | 11 | 15 | 4 | 7 | 9 |
| $M_{2m}$ | 10 | 12 | 15 | 7 | 7 | 10 |

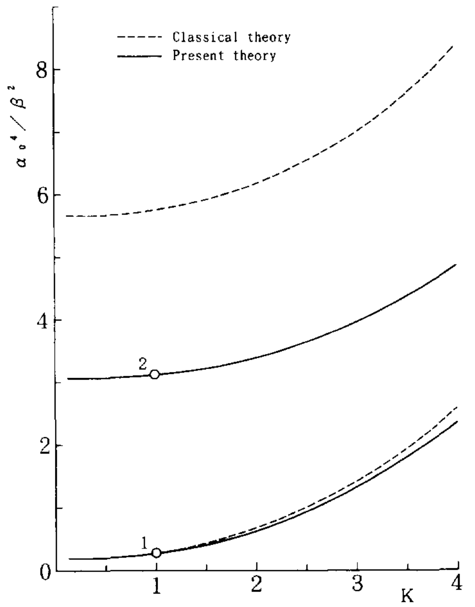


Fig. 4. Frequency curves, (S-S) modes ($\beta = 6.0$) $N = 3$ (90°, 0°, 90°), $\mu_0 = 0.2$.

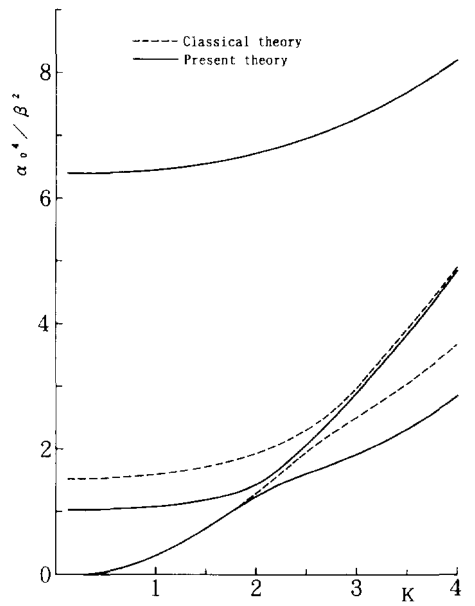


Fig. 5. Frequency curves, (S-A) modes ($\beta = 6.0$) $N = 3$ (90°, 0°, 90°), $\mu_0 = 0.2$.

the present theory are always below those for the classical theory. Of course, for $\beta = r_0/h = 6$, the shell is moderately thick, so some significant differences between the results of the present thick shell theory and those of classical (thin) shell theory may be expected. But Figs 4–7 show great differences between the frequencies obtained from the two theories in some places. These large differences are partly due to the strong orthotropy of the graphite-epoxy material being used. The difference between both the theories typically increases as $\beta$ decreases, or as $K(=m\pi r_0/l)$ becomes large, or as the vibration mode becomes higher. As seen from Figs 5 and 6, curve veerings (cf. Leissa, 1974) are occurring in the first and second mode frequency curves. In the case of the (S-S) mode in Fig. 4, the difference between both the theories is very large for the second mode. As for the (S-A) and (A-S) modes in Figs 5 and 6, the difference for the third mode becomes large. In the (A-A) mode in Fig. 7, the difference is large for the second mode.

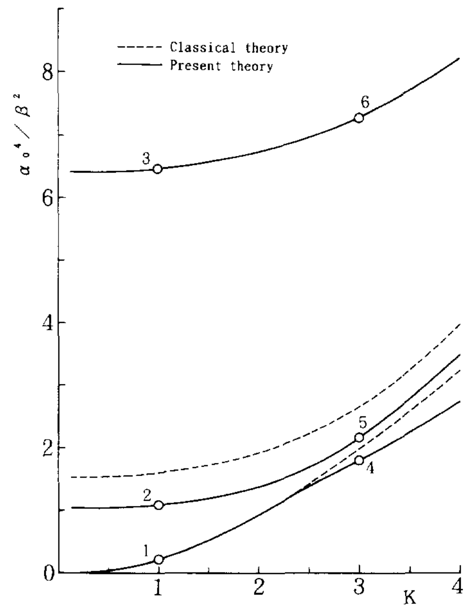


Fig. 6. Frequency curves, (A-S) modes ($\beta = 6.0$) $N = 3$ (90°, 0°, 90°), $\mu_0 = 0.2$.

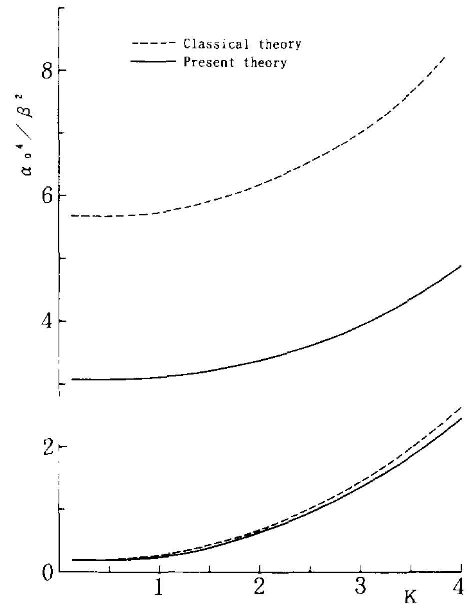


Fig. 7. Frequency curves, (A-A) modes ($\beta = 6.0$) $N = 3$ (90°, 0°, 90°), $\mu_0 = 0.2$.

Figures 8 and 9 show the frequency curves of elliptical cylindrical shells with stacking sequence (0°, 90°, 0°). The curves are generally lower compared with those for shells with stacking sequence (90°, 0°, 90°). But the differences between the data of the present and the classical (Suzuki *et al.*, 1994) theories are similar.

Figure 10 depicts the mode shapes for the numbered points on the frequency curves in Figs 4 and 6. They are the displacements $w_m$ for $0 \leqslant \theta \leqslant \pi/2$, in which the maximum amplitude is taken to be unity. From Fig. 10 (a) one finds that the mode shapes of points 1 and 2 in Fig. 4 are very similar to the $\cos 2\theta$ and $\cos 4\theta$ modes of the circular cylindrical shells, respectively, and from Fig. 10(b) one finds that the mode shapes of point 1, 2 and 3 in Fig. 6 are very similar to the $\sin\theta$, $\sin 3\theta$ and $\sin 5\theta$ modes of the circular cylindrical shells, respectively. There is a transition of mode shapes in the region of veering in Fig. 6. The mode shape of point 4 is similar to that of point 2 and the mode shape of point 5 to that of point 1, although the amplitudes are different to each other. The points 6 and 3 in

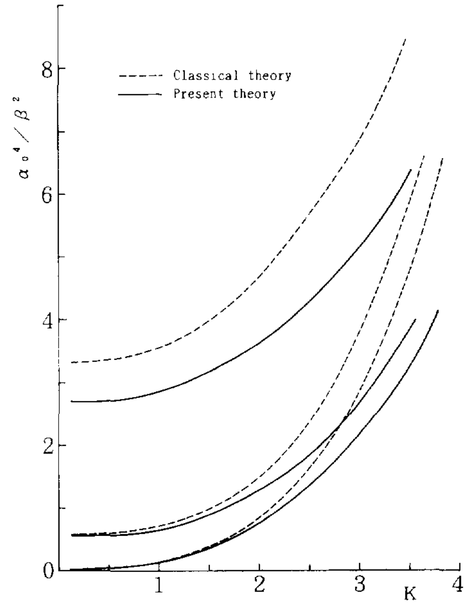


Fig. 8. Frequency curves, (S-S) modes ($\beta = 6.0$) $N = 3$ (0°, 90°, 0°), $\mu_0 = 0.2$.

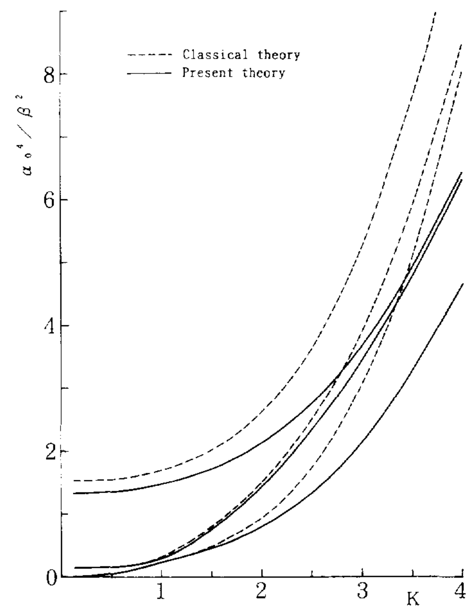


Fig. 9. Frequency curves, (S-A) modes ($\beta = 6.0$) $N = 3$ (0°, 90°, 0°), $\mu_0 = 0.2$.

Fig. 6 are on the same frequency curve and the mode shapes of points 6 and 3 are very similar. The (A-A) and (S-A) modes in the case where $\mu_0 = 0.2$ are very similar to the (S-S) and (A-S) modes, respectively, which are omitted in this work.

Tables 2–5 show the effects of ellipticity $\mu_0$ upon the frequencies. In the tables blanks represent that the frequencies cannot be found because of computational limitations. One finds that the computational limits of the present methods is up to the $\mu_0 = 0.4$ ($\sim a/b = 1.53$). Examining Tables 2–5, one sees that the effects of increasing ellipticity is to increase some frequencies, but decrease others. In studying the geometry of the mode shapes one can see that if there were no ellipticity ($\mu_0 = 0$), which corresponds to a circular cylindrical shell, the S-S and A-A mode shapes would be described by $\cos n\theta$ and $\sin n\theta$ variations in $w_m$, respectively, with $n = 2, 4, 6, \cdots$, whereas the S-A and A-S modes would correspond to $\cos n\theta$ and $\sin n\theta$ with $n = 1, 3, 5, \cdots$. In this case ($\mu_0 = 0$) the S-S and A-A modes would be degenerate (i.e., having the same frequencies), as would the S-A and A-S

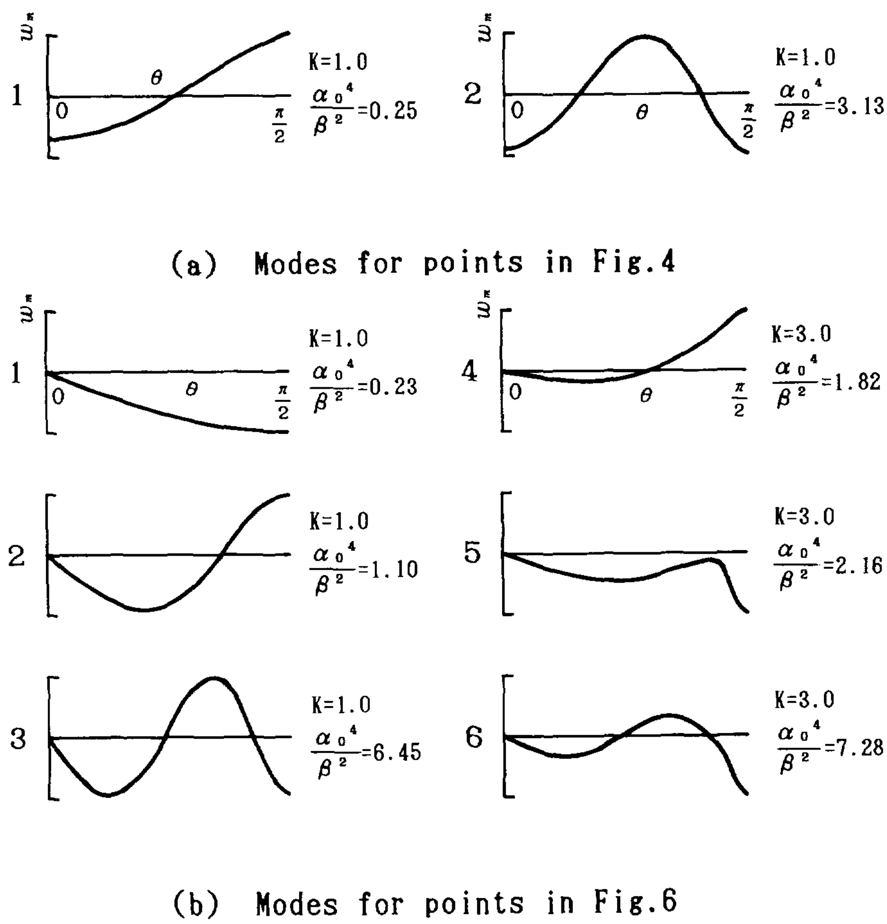


Fig. 10. Mode shapes. (a) Modes for points in Fig. 4. (b) Modes for points in Fig. 6.

Table 2. Effects of the ellipticity $\mu_0$ upon the frequencies $\alpha_0^4/\beta^2$, $N = 3$ (90°, 0°, 90°), $\beta = 6.0$, (S-S) modes

| $K$ | Mode | $\mu_0 = 0.1$ | 0.2 | 0.3 | 0.4 |
|---|---|---|---|---|---|
| 0.5 | 1st | 0.172 | 0.171 | 0.169 | 0.167 |
| | 2nd | 3.085 | 3.079 | 3.069 | 3.054 |
| 1.0 | 1st | 0.253 | 0.248 | 0.241 | 0.232 |
| | 2nd | 3.129 | 3.125 | 3.116 | 3.101 |
| 2.0 | 1st | 0.660 | 0.639 | 0.606 | 0.562 |
| | 2nd | 3.394 | 3.390 | 3.381 | 3.363 |
| 3.0 | 1st | 1.386 | 1.331 | 1.248 | 1.144 |
| | 2nd | 3.944 | 3.944 | 3.935 | 3.909 |

modes. For small (but nonzero) $\mu_0$ the degenerate frequencies are distinct, but close to each other, as may be seen by comparing Tables 2 and 5, or Tables 3 and 4.

Figure 11 shows the effects of number of laminae and stacking sequence upon the frequencies for (S-S) modes of shells with the length ratio $K(=m\pi r_0/l) = 2$ in the case where $\beta = 6$ and $\mu_0 = 0.2$. As seen from the figures, there are large differences between the data for stacking sequence (0°, 90°, 0° $\cdots$) and (90°, 0°, 90° $\cdots$) when $N$ is small, but the differences become smaller with an increasing number of laminae. It is interesting to note that, for both types of stacking sequences, some frequencies increase while others decrease as the number of layers ($N$) increases.

Table 6 shows the effects of various choices of elastic constants upon the frequencies. Generally, for the results presented in this paper, the elastic constants are taken as in case

Table 3. Effects of the ellipticity $\mu_0$ upon the frequencies $\alpha_0^4/\beta^2$, $N = 3$ (90°, 0°, 90°), $\beta = 6.0$, (S-A) modes

| $K$ | Mode | $\mu_0 = 0.1$ | 0.2 | 0.3 | 0.4 |
|---|---|---|---|---|---|
| | 1st | 0.053 | 0.056 | 0.060 | 0.063 |
| 0.5 | 2nd | 1.056 | 1.050 | 1.041 | 1.029 |
| | 3rd | 6.403 | 6.405 | 6.407 | — |
| | 1st | 0.288 | 0.307 | 0.326 | 0.345 |
| 1.0 | 2nd | 1.105 | 1.099 | 1.089 | 1.075 |
| | 3rd | 6.450 | 6.455 | 6.459 | 6.460 |
| | 1st | 1.217 | 1.267 | 1.272 | — |
| 2.0 | 2nd | 1.403 | 1.437 | 1.509 | 1.598 |
| | 3rd | 6.714 | 6.720 | 6.726 | 6.728 |
| | 1st | 1.963 | 1.921 | 1.865 | 1.800 |
| 3.0 | 2nd | 2.663 | 2.916 | 3.179 | 3.446 |
| | 3rd | 7.266 | 7.275 | 7.286 | 7.308 |

Table 4. Effects of the ellipticity $\mu_0$ upon the frequencies $\alpha_0^4/\beta^2$, $N = 3$ (90°, 0°, 90°), $\beta = 6.0$, (A-S) modes

| $K$ | Mode | $\mu_0 = 0.1$ | 0.2 | 0.3 | 0.4 |
|---|---|---|---|---|---|
| | 1st | 0.046 | 0.042 | 0.038 | 0.034 |
| 0.5 | 2nd | 1.056 | 1.050 | 1.041 | 1.028 |
| | 3rd | 6.403 | 6.405 | 6.405 | — |
| | 1st | 0.247 | 0.226 | 0.204 | 0.182 |
| 1.0 | 2nd | 1.105 | 1.099 | 1.089 | 1.076 |
| | 3rd | 6.450 | 6.454 | 6.458 | — |
| | 1st | 1.037 | 0.938 | 0.838 | 0.737 |
| 2.0 | 2nd | 1.399 | 1.397 | 1.391 | 1.377 |
| | 3rd | 6.714 | 6.720 | 6.725 | — |
| | 1st | 1.947 | 1.816 | 1.632 | 1.439 |
| 3.0 | 2nd | 2.250 | 2.164 | 2.129 | 2.098 |
| | 3rd | 7.266 | 7.275 | 7.286 | — |

Table 5. Effects of the ellipticity $\mu_0$ upon the frequencies $\alpha_0^4/\beta^2$, $N = 3$ (90°, 0°, 90°), $\beta = 6.0$, (A-A) modes

| $K$ | Mode | $\mu_0 = 0.1$ | 0.2 | 0.3 | 0.4 |
|---|---|---|---|---|---|
| 0.5 | 1st | 0.179 | 0.192 | 0.208 | 0.227 |
| | 2nd | 3.085 | 3.080 | 3.073 | 3.066 |
| 1.0 | 1st | 0.253 | 0.250 | 0.245 | 0.237 |
| | 2nd | 3.129 | 3.126 | 3.120 | 3.115 |
| 2.0 | 1st | 0.664 | 0.654 | 0.638 | 0.615 |
| | 2nd | 3.394 | 3.392 | 3.392 | |
| 3.0 | 1st | 1.398 | 1.375 | 1.337 | 1.285 |
| | 2nd | 3.944 | 3.947 | 3.949 | — |

I. In case II the effects of changing of $G_{23}$ upon the frequencies are examined. In the table, $\kappa = \pi^2/12$ is the shear coefficient, which was used by Mirsky and Herrmann (1957, 1964) for isotropic, homogeneous, circular thick cylindrical shells. One finds that the frequencies are reduced as $G_{23}$ is diminished by $\kappa$. The cases III and IV arise when the stress-strain relations between ($\sigma_{xx}$, $\sigma_{\theta\theta}$, $\sigma_{x\theta}$) and ($\varepsilon_{xx}$, $\varepsilon_{\theta\theta}$, $\varepsilon_{x\theta}$) of eqn (5) are replaced by those of two dimensional shell theory. From the results, it is seen that the case IV gives the lowest frequencies among the four cases.

## 4. CONCLUSIONS

In this paper, an exact solution procedure has been demonstrated for solving free vibration problems for laminated composite, noncircular thick cylindrical shells. The

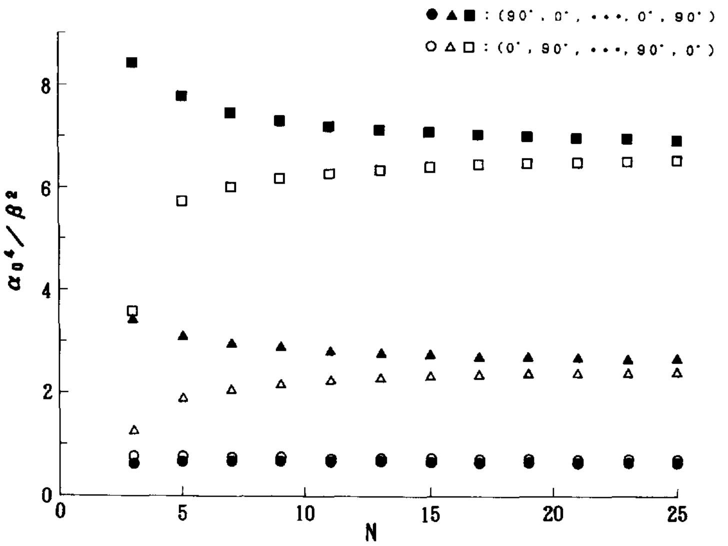


Fig. 11. Effect of number of layers upon the frequencies, (S-S) modes ($\beta = 6.0$, $K = 2.0$, $\mu_0 = 0.2$).

Table 6. Effects of the moduli of elasticity upon the frequencies $\alpha_0^4/\beta^2$, (S-S) modes, $N = 3$ (0°, 90°, 0°), $\beta = 6.0$, $\mu_0 = 0.2$

| $K$ | Mode | Classical theory | Case I | Case II | Case III | Case IV |
|---|---|---|---|---|---|---|
| | 1st | 0.146 | 0.145 | 0.145 | 0.142 | 0.142 |
| 1.0 | 2nd | 0.720 | 0.667 | 0.661 | 0.629 | 0.624 |
| | 3rd | 3.569 | 2.864 | 2.812 | 2.713 | 2.666 |
| | 1st | 0.843 | 0.767 | 0.764 | 0.758 | 0.755 |
| 2.0 | 2nd | 1.485 | 1.274 | 1.247 | 1.208 | 1.202 |
| | 3rd | 4.686 | 3.593 | 3.528 | 3.419 | 3.362 |
| | 1st | 2.875 | 2.208 | 2.185 | 2.176 | 2.163 |
| 3.0 | 2nd | 3.783 | 2.700 | 2.677 | 2.628 | 2.609 |
| | 3rd | 5.950 | 5.185 | 5.084 | 5.067 | 4.890 |

Case I: $G_{23} = 3.45$ (GPa), $\nu_{12} = \nu_{13} = \nu_{23} = 0.3$.
Case II: $G_{23} = \kappa \times 3.45$ (GPa), $\nu_{12} = \nu_{13} = \nu_{23} = 0.3$.
Case III: $G_{23} = 3.45$ (GPa), $\nu_{12} = 0.3$ and $\nu_{13} = \nu_{23} = 0$.
Case IV: $G_{23} = \kappa \times 3.45$ (GPa), $\nu_{12} = 0.3$ and $\nu_{13} = \nu_{23} = 0$.

method is a general one applicable to various noncircular thick cylindrical shells, although limited to crossply shells having both ends freely supported. As numerical examples, natural frequencies were found for symmetrically laminated, elliptical cylindrical shells, and from the results were clarified the effects of the shear deformation and rotary inertia upon the frequencies.

Although the procedure has been carried out in detail only for symmetrically laminated shells, it may also be applied to unsymmetric laminates. In this case not all the elastic (bending-stretching) stiffness coefficients ($B_{ij}$) in eqns (15) would be zero, and the algebraic complexity of the resulting algebraic equations would be somewhat increased.

Similarly, although the procedure is demonstrated only for shell cross-sections having at least one axis of symmetry, it may be generalized to general (unsymmetric) cross-sections by expanding $\Phi^2$ of eqn (24) in all powers of $\theta$. However, this would require enforcing ten continuity conditions for displacements, bending slope, forces and moments at a reference point taken on the shell, instead of the five boundary conditions (eqns (32) or (33)) which are applied at the point on a symmetry axis.

## REFERENCES

Leissa, A. W. (1974). On a curve veering aberration. *ZAMP* **25**, 99–111.
Love, A. E. H. (1927). *A Treatise on the Mechanical Theory of Elasticity*. Cambridge University Press.

Mirsky, I. and Herrmann, G. (1957). Nonaxially symmetric motions of cylindrical shells. *J. Acoust. Soc. Am.* **29,** 1116–1123.

Mirsky, I. (1964). Vibration of orthotropic thick cylindrical shells. *J. Acoust. Soc. Am.* **36,** 41–51.

Qatu, M. S. and Leissa, A. W. (1991a). Natural frequencies for cantilevered doubly-curved laminated composite shallow shells. *Comp. Struct.* **17,** 227–255.

Qatu, M. S. and Leissa, A. W. (1991b). Free vibrations of completely free doubly curved laminated composite shallow shells. *J. Sound Vib.* **151,** 9–29.

Singh, A. V., Zhu, L. and Mirza, S. (1991). On asymmetric vibrations of layered orthotropic shells of revolution. *J. Sound Vib.* **148,** 265–277.

Sivadas, K. R. and Ganesan, N. (1991). Vibration analysis of laminated conical shells with variable thickness. *J. Sound Vib.* **148,** 477–491.

Suzuki, K., Takahashi, S. and Ishiyama, H. (1978). In-plane vibrations of curved bars. *Bull. JSME.* **21,** 618–627.

Suzuki, K. and Leissa, A. W. (1985). Free vibrations of non-circular cylindrical shells having circumferentially varying thickness. *J. Appl. Mech.* **52,** 149–154.

Suzuki, K. and Leissa, A. W. (1986). Exact solutions for the free vibrations of open cylindrical shells with circumferentially varying curvature and thickness. *J. Sound Vib.* **107,** 1–15.

Suzuki, K. and Leissa, A. W. (1990). Analysis of free vibrations of noncircular thick cylindrical shells having circumferentially varying thickness. *Int. J. Solids Structures* **26,** 255–270.

Suzuki, K., Shikanai, G. and Leissa, A. W. (1994). Free vibrations of laminated composite noncircular thin cylindrical shells. *J. Appl. Mech.* **61,** 861–871.

Vinson, J. R. and Sierakowski, R. L. (1987). *The Behaviour of Structures Composed of Composite Materials*, Martinus Nijhoff Publishers, Dordrecht, The Netherlands.

Whitney, J. M. (1987). *Structural Analysis of Laminated Anisotropic Plates*, Technomic Publishing Co., Lancaster, Pennsylvania.

## APPENDIX A: $\bar{Q}_{ij}$ IN EQNS (5)

$$
\begin{aligned}
\bar{Q}_{11} &= Q_{11}m^4 + 2(Q_{12} + 2Q_{66})m^2n^2 + Q_{22}n^4, \\
\bar{Q}_{12} &= (Q_{11} + Q_{22} - 4Q_{66})m^2n^2 + Q_{12}(m^4 + n^4), \\
\bar{Q}_{16} &= -mn^3Q_{22} + m^3nQ_{11} - mn(m^2 - n^2)(Q_{12} + 2Q_{66}), \\
\bar{Q}_{22} &= Q_{11}n^4 + 2(Q_{12} + 2Q_{66})m^2n^2 + Q_{22}m^4, \\
\bar{Q}_{26} &= -m^3nQ_{22} + mn^3Q_{11} + mn(m^2 - n^2)(Q_{12} + 2Q_{66}), \\
\bar{Q}_{44} &= Q_{44}m^2 + Q_{55}n^2, \\
\bar{Q}_{45} &= (Q_{55} - Q_{44})mn, \\
\bar{Q}_{55} &= Q_{55}m^2 + Q_{44}n^2, \\
\bar{Q}_{66} &= (Q_{11} + Q_{22} - 2Q_{12})m^2n^2 + Q_{66}(m^2 - n^2)^2, \\
m &= \cos\varphi_0, \quad n = \sin\varphi_0, \\
Q_{11} &= E_{11}(1 - \nu_{23}\nu_{32})/\Delta, \\
Q_{22} &= E_{22}(1 - \nu_{31}\nu_{13})/\Delta, \\
Q_{12} &= E_{11}(\nu_{21} + \nu_{31}\nu_{23})/\Delta = E_{22}(\nu_{12} + \nu_{32}\nu_{13})/\Delta, \\
Q_{44} &= G_{23}, \quad Q_{55} = G_{13}, \quad Q_{66} = G_{12}, \\
\Delta &= 1 - \nu_{12}\nu_{21} - \nu_{23}\nu_{32} - \nu_{31}\nu_{13} - 2\nu_{21}\nu_{32}\nu_{13},
\end{aligned}
$$

where $E_{11}$ is the modulus of elasticity of the lamina in the direction of the fibers and $E_{22}$ is the transverse modulus; $G_{12}$, $G_{13}$ and $G_{23}$ are the shear moduli; and $\nu_{12}$, $\nu_{21}$, $\nu_{13}$, $\nu_{31}$, $\nu_{23}$ and $\nu_{32}$ are Poisson's ratios.

The principal material axes are labelled 1 and 2; that is, the 1 direction is parallel to the fibers, and the 2 direction is normal to them. The shell geometric axes are $x$ and $\theta$ as depicted in Fig. A.1.

## APPENDIX B: TERMS CONTAINED IN EQNS (28) AND (30)

For eqn (28)

$$
\begin{aligned}
f_{na} = {} & (\alpha_0^4\bar{\rho}_1 - K^2\beta^2A_{11})A_n + K\beta^2G(2n+1)(A_{12} + A_{66})B_n + K\beta^2GA_{12}C_n + G\left(\frac{\alpha_0^4}{\beta^2}\bar{\rho}_3 - K^2D_{11}\right)D_n \\
& + G^2\Phi_0(2n+1)\left[\beta^2A_{66}\sum_{p=0}^{n}(n+p+1)\eta_{n+1-p}A_p - GD_{66}\sum_{p=0}^{n-1}\eta_{n-p}(2p+2)(D_{p+1} - G\Phi_0\eta_0A_{p+1})\right. \\
& \left. + G^2\Phi_0D_{66}\sum_{q=0}^{n}\eta_{n-q}\sum_{p=0}^{q}(q+p+1)\eta_{q+1-p}A_p\right]
\end{aligned}
$$

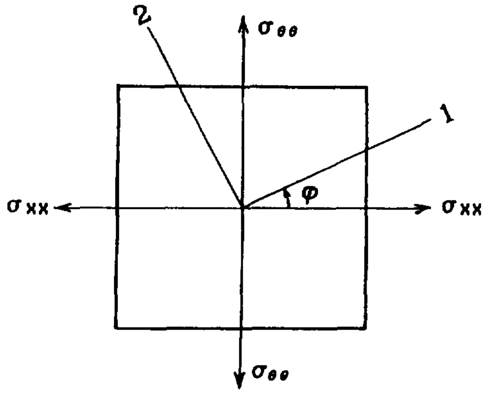


Fig. A.1. Coordinate system of lamina.

$$f_{nb} = (\alpha_0^4\bar{\rho}_1 - K^2\beta^2 A_{66})B_n + G^4\Phi_0^2\eta_0^2(2n+2)D_{22}C_{n+1} + G\Phi_0\sum_{p=0}^{n}\eta_{n-p}F_p\left(\frac{\alpha_0^4}{\beta^2}\bar{\rho}_3 + \beta^2 A_{44} - K^2 D_{66}\right)$$

$$+\sum_{p=0}^{n}[\beta^2 G^2\Phi_0 A_{44}\eta_{n-p}\{(2p+2)C_{p-1} - B_p\} + \beta^2 G^2\Phi_0(n+p+1)(2p+1)\eta_{n+1-p}A_{22}B_p]$$

$$+\sum_{p=0}^{n} D_{22}G^3\Phi_0^2\eta_0(2n+2)\eta_{n+1-p}[G\{(2p+1)B_p + C_p\} - (n+p+2)F_p]$$

$$+G^3\Phi_0^2 D_{44}\sum_{q=0}^{n}\eta_{n-q}\sum_{p=0}^{q}\eta_{q-p}[G\{(2p+2)C_{p+1} - B_p\} + F_p]$$

$$+G^3\Phi_0^2 D_{22}\sum_{q=0}^{n}(n+q+1)\eta_{n-1-q}\sum_{p=0}^{q}\eta_{q-p}[G\{(2p+1)B_p + C_p\} - (q+p+1)F_p]$$

$$-\beta^2 G\Phi_0\sum_{p=0}^{n-1}(n+p+1)\eta_{n+1-p}[K(A_{66}+A_{12})A_p - GA_{22}C_p]$$

$$f_{nc} = (\alpha_0^4\bar{\rho}_1 - K^2\beta^2 A_{55})C_n - K\beta^2 A_{55}D_n + G\Phi_0\eta_0(\beta^2 A_{44} + G^2\Phi_0\eta_0 D_{44})(2n+1)(F_n - GB_n)$$

$$-\beta^2 G\Phi_0\sum_{p=0}^{n}\eta_{n-p}[-KA_{12}A_p + GA_{22}\{(2p+1)B_p + C_p\}]$$

$$+G\Phi_0(\beta^2 A_{44} + G^2\Phi_0\eta_0 D_{44})\sum_{p=0}^{n-1}(n+p+1)\eta_{n-p}[G\{(2p+2)C_{p+1} - B_p\} + F_p]$$

$$-D_{22}G^3\Phi_0^2\sum_{q=0}^{n}\eta_{n-q}\sum_{p=0}^{q}\eta_{q-p}[G\{(2p+1)B_p + C_p\} - (q+p+1)F_p]$$

$$+D_{44}G^3\Phi_0^2\sum_{q=0}^{n}(n+q+1)\eta_{n-q}\sum_{p=0}^{q-1}\eta_{q-p}[G\{(2p+2)C_{p+1} - B_p\} + F_p]$$

$$f_{nd} = -\beta^2 KA_{55}C_n + D_n\left(\frac{\alpha_0^4}{\beta^2}\bar{\rho}_3 - K^2 D_{11} - \beta^2 A_{55}\right) + KG\Phi_0\eta_0(2n+1)D_{66}F_n$$

$$+G\Phi_0\sum_{p=0}^{n}\eta_{n-p}\left[\left(\frac{\alpha_0^4}{\beta^2}\bar{\rho}_3 - K^2 D_{11}\right)A_p + K(n+p+1)D_{12}F_p\right]$$

$$+G\Phi_0 D_{66}\sum_{p=0}^{n-1}(n+p+1)\eta_{n-p}[KF_p + G(2p+2)D_{p+1} - G^2\Phi_0\eta_0(2p+2)A_{p+1}]$$

$$-G^3\Phi_0^2 D_{66}\sum_{q=0}^{n}(n+q+1)\eta_{n-q}\sum_{p=0}^{q}(q+p+1)\eta_{q-1-p}A_p$$

$$f_{ne} = GB_n\left(\frac{\alpha_0^4}{\beta^2}\bar{\rho}_3 + \beta^2 A_{44} - K^2 D_{66}\right) + F_n\left(\frac{\alpha_0^4}{\beta^2}\bar{\rho}_3 - \beta^2 A_{44} - K^2 D_{66}\right)$$

$$-G(2n+2)C_{n+1}(\beta^2 A_{44} + G^2\Phi_0\eta_0 D_{22}) - KG(2n+2)(D_{66}+D_{12})D_{n+1}$$

$$-G^2\Phi_0 D_{44}\sum_{p=0}^{n}\eta_{n-p}[G\{(2p+2)C_{p+1} - B_p\} + F_p]$$

$$-G^2\Phi_0(2n+2)D_{22}\sum_{p=0}^{n}\eta_{n+1-p}[G\{(2p+1)B_p + C_p\} - (n+p+2)F_p]$$

for eqn (30)

$$f_{na}=(\alpha_0^4\bar{\rho}_1-K^2\beta^2A_{11})A_n+K\beta^2GA_{12}C_n+G\left(\frac{\alpha_0^4}{\beta^2}\bar{\rho}_3-K^2D_{11}\right)D_n+K\beta^2G(2n+2)(A_{66}+A_{12})B_{n+1}$$

$$+G^2\Phi_0(2n+2)\sum_{p=0}^{n}[(\beta^2A_{66}+G^2\Phi_0\eta_0D_{66})(n+p+2)\eta_{n+1-p}A_p-GD_{66}(2p+1)\eta_{n+1-p}D_p]$$

$$+G^4\Phi_0^2(2n+2)D_{66}\sum_{q=0}^{n}\eta_{n+1-q}\sum_{p=0}^{q}(q+p+1)\eta_{q-p}A_p$$

$$f_{nb}=-K\beta^2G\Phi_0\eta_0(2n+1)A_{12}A_n+(\alpha_0^4\bar{\rho}_1-K^2\beta^2A_{66})B_n+G^2\Phi_0\eta_0(2n+1)(\beta^2A_{22}+G^2\Phi_0\eta_0D_{22})C_n$$

$$+G\Phi_0\sum_{p=0}^{n}\eta_{n-p}\left[\left(\frac{\alpha_0^4}{\beta^2}\bar{\rho}_3+\beta^2A_{44}-K^2D_{66}\right)F_p-K\beta^2A_{66}(n+p+1)A_p+\beta^2GA_{44}\{-B_p+(2p+1)C_p\}\right]$$

$$+G\Phi_0\sum_{p=0}^{n-1}(n+p+1)\eta_{n-p}[G(\beta^2A_{22}+G^2\Phi_0\eta_0D_{22})\{(2p+2)B_{p+1}+C_p\}-K\beta^2A_{12}A_p$$

$$-G^2\Phi_0\eta_0D_{22}(2p+2)F_{p+1}]+G^3\Phi_0^2D_{44}\sum_{q=0}^{n}\eta_{n-q}\sum_{p=0}^{q}\eta_{q-p}[G\{-B_p+(2p+1)C_p\}-F_p]$$

$$+G^3\Phi_0^2D_{22}\sum_{q=0}^{n}(n+q+1)\eta_{n-q}\left[G\sum_{p=0}^{q-1}\eta_{q-p}\{(2p+2)B_{p+1}+C_p\}-\sum_{p=0}^{q}(q+p+1)\eta_{q+1-p}F_p\right]$$

$$f_{nc}=(\alpha_0^4\bar{\rho}_1-K^2\beta^2A_{55})C_n-K\beta^2A_{55}D_n+G\Phi_0\eta_0(2n+2)(\beta^2A_{44}+G^2\Phi_0\eta_0D_{44})(F_{n+1}-GB_{n+1})$$

$$+G\Phi_0\sum_{p=0}^{n}\eta_{n+1-p}[\![\{\beta^2A_{44}(n+p+1)+G^2\Phi_0\eta_0(2n+2)D_{44}\}[G\{-B_p+(2p+1)C_p\}+F_p]]\!]$$

$$-G\Phi_0\beta^2\sum_{p=0}^{n}\eta_{n-p}[-KA_{12}A_p+GA_{22}\{(2p+2)B_{p+1}+C_p\}]$$

$$-G^3\Phi_0^2D_{22}\sum_{q=0}^{n}\eta_{n-q}\left[G\sum_{p=0}^{q}\eta_{q-p}\{(2p+2)B_{p+1}+C_p\}-\sum_{p=0}^{q+1}(q+p+1)\eta_{q+1-p}F_p\right]$$

$$+G^3\Phi_0^2D_{44}\sum_{q=0}^{n}(n+q+1)\eta_{n+1-q}\sum_{p=0}^{q}\eta_{q-p}[G\{-B_p+(2p+1)C_p\}+F_p]$$

$$f_{nd}=-K\beta^2A_{55}C_n+\left(\frac{\alpha_0^4}{\beta^2}\bar{\rho}_3-\beta^2A_{55}-K^2D_{11}\right)D_n+KG\Phi_0\eta_0(2n+2)(D_{66}+D_{12})F_{n+1}$$

$$+G\Phi_0\sum_{p=0}^{n}\left[\left(\frac{\alpha_0^4}{\beta^2}\bar{\rho}_3-K^2D_{11}\right)\eta_{n-p}A_p-G^2\Phi_0\eta_0(2n+2)(n+p+2)\eta_{n+1-p}D_{66}A_p\right.$$

$$\left.+(n+p+1)\eta_{n+1-p}\{K(D_{12}+D_{66})F_p+G(2p+1)D_{66}D_p\}\right]$$

$$-G^3\Phi_0^2D_{66}\sum_{q=0}^{n}(n+q+1)\eta_{n+1-q}\sum_{p=0}^{q}(q+p+1)\eta_{q-p}A_p$$

$$f_{ne}=GB_n\left(\frac{\alpha_0^4}{\beta^2}\bar{\rho}_3+\beta^2A_{44}-K^2D_{66}\right)-GC_n(2n+1)(\beta^2A_{44}+G^2\Phi_0\eta_0D_{22})$$

$$-KG(2n+1)(D_{12}+D_{66})D_n+\left(\frac{\alpha_0^4}{\beta^2}\bar{\rho}_3-\beta^2A_{44}-K^2D_{66}\right)F_n$$

$$+G^2\Phi_0\sum_{p=0}^{n}[\{(2n+1)D_{22}(n+p+1)\eta_{n+1-p}-D_{44}\eta_{n-q}\}F_p-GD_{44}\eta_{n-p}\{-B_p+(2p+1)C_p\}]$$

$$-G^3\Phi_0(2n+1)D_{22}\sum_{p=0}^{n-1}\eta_{n-p}\{(2p+2)B_{p+1}+C_p\}$$